



# Advanced Synthesis & Catalysis

## Accepted Article

**Title:** Gold(I) Complexes with Eight-Membered NHC Ligands:  
Synthesis, Structures and Catalytic Activity

**Authors:** Alejandro Cervantes-Reyes, Frank Rominger, Matthias  
Rudolph, and A. Stephen K. Hashmi

This manuscript has been accepted after peer review and appears as an Accepted Article online prior to editing, proofing, and formal publication of the final Version of Record (VoR). This work is currently citable by using the Digital Object Identifier (DOI) given below. The VoR will be published online in Early View as soon as possible and may be different to this Accepted Article as a result of editing. Readers should obtain the VoR from the journal website shown below when it is published to ensure accuracy of information. The authors are responsible for the content of this Accepted Article.

**To be cited as:** *Adv. Synth. Catal.* 10.1002/adsc.202000281

**Link to VoR:** <http://dx.doi.org/10.1002/adsc.202000281>

# Gold(I) Complexes with Eight-Membered NHC Ligands: Synthesis, Structures and Catalytic Activity

Alejandro Cervantes-Reyes,<sup>a</sup> Frank Rominger,<sup>a,†</sup> Matthias Rudolph,<sup>a</sup> and A. Stephen K. Hashmi<sup>a,b,\*</sup>

<sup>a</sup> Organisch-Chemisches Institut, Heidelberg University, Im Neuenheimer Feld 270, 69120 Heidelberg, Germany  
Fax: (+49)-6221-54-4205

E-mail: hashmi@hashmi.de

<sup>b</sup> Chemistry Department, Faculty of Science, King Abdulaziz University, Jeddah 21589, Saudi Arabia

<sup>†</sup> Crystallographic investigation

Received: ((will be filled in by the editorial staff))



Supporting information for this article is available on the WWW under <http://dx.doi.org/10.1002/adsc.201#####>. ((Please delete if not appropriate))

**Abstract.** A series of expanded-ring NHC gold complexes of the formula (NaphtDHD-Ar)Au-X (NaphtDHD = 4,5-dihydro-1*H*-naphtho[1,8-*ef*][1,3]diazocin-3(2*H*)-ylidene; Ar: Mes = 2,4,6-trimethylphenyl, Dipp = 2,6-diisopropylphenyl or Xyl = 2,6-dimethylphenyl; X = Cl, NCCH<sub>3</sub>, NTf<sub>2</sub>) have been synthesized, including the first gold(I) triflimidate complex (**5**) stabilized by an eight-membered NHC ligand. The new organogold compounds have been characterized by mass spectrometry, IR spectroscopy, and <sup>1</sup>H and <sup>13</sup>C NMR spectroscopy. The structural geometries of **3b–c** and **5** have been unequivocally established by crystallographic analysis revealing broad N-C-N angles (>121°) and high buried volume values (46–54%).

The first catalytic studies were carried out on the cycloisomerization of 1,6-enynes, obtaining full conversions (0.5 mol% catalyst loading) and excellent *endo/exo* selectivity (up to 99:1), and on the gold-catalyzed phenol synthesis. Lastly, the (NaphtDHD-Dipp)Au<sup>+</sup> NTf<sub>2</sub><sup>−</sup> species was subjected to a kinetic experiment in the cyclization of *N*-propargyl carboxamide to evaluate the efficiency of the pre-formed catalyst (**5**) and the in situ activated gold complex (**3b** + AgNTf<sub>2</sub>).

**Keywords:** Enynes; Expanded Ring NHC Ligands; Gold; Heterocycles

## Introduction

N-heterocyclic carbenes (NHCs)<sup>[1]</sup> are efficient stabilizing ligands for metals owing to their steric and electronic features which can be modulated either from the substituents at the N-atoms or from the alkyl/aryl backbones.<sup>[2,3]</sup> In this context, expanded-ring backbone NHCs turn out to increase the steric environment around the first coordination sphere of the metal, where the catalysis occurs.<sup>[4,5]</sup>

Since the pioneering work of Cavell *et al.*, the interest in expanded-ring NHC-Au(I) complexes has surged due to their widespread applications, particularly in homogeneous catalysis.<sup>[6–8]</sup> It has been established, that this class of ligands can efficiently stabilize  $\pi$ -acidic gold cations by increasing the ionic character of the complex, leading to an increased catalytic activity. Furthermore, the stereoelectronic features of the NHC ligands can be tuned to obtain the desired selectivity.<sup>[9,10]</sup>

Several examples of six- and seven-membered NHC-Au(I) complexes have been reported, as well as their structural and catalytic properties.<sup>[11]</sup> In addition, a large family of eight-membered NHC metal

complexes (where metal is different from gold) have been reported.<sup>[12]</sup>

During the preparation of this paper, Huynh and co-workers reportedly synthesized some alkyl-chain backbone eight-membered NHC gold(I)-bromide complexes.<sup>[5d,13]</sup> Recently, we have developed the first examples of sterically bulky nine- and ten-membered NHC ligands and the synthesis of the corresponding gold complexes. The catalytic activity of these species was tested down to a 50 ppm catalyst loading and an outstanding performance (TON = 3800) was observed for the cyclization of an *N*-arylpropargylamide.<sup>[14]</sup> In virtue of those findings we were interested in further expanding the chemistry of expanded-ring NHC-Au(I) complexes.

Herein, the synthesis, full characterization and steric profiles of neutral and cationic eight-membered NHC-Au(I) complexes is presented, along with a preliminary catalytic survey of several synthetically relevant cyclization reactions, including the cycloisomerization of 1,6-enynes and the gold-catalyzed oxazole synthesis.

## Results and Discussion

### Synthesis of NHC-Au(I) complexes

The first report of the 4,5-dihydro-1*H*-naphtho[1,8-*ef*][1,3]diazocin-3(2*H*)-ylidene (NaphtDHD) NHC ligand and the corresponding NHC-AgBr complexes was made by Nechaev *et al.* and the access to the NHC-CuBr complexes was accomplished by ligand transfer from the isostructural Ag(I) compounds.<sup>[12c]</sup> As a direct synthetic pathway to the current NHC-AuCl complexes, we considered the generation of the free NHC in solution by deprotonation of a suitable NHC-HX salt (*i.e.* X = BF<sub>4</sub>) as carbene precursor, followed by direct complexation with a gold source (*i.e.* (SMe<sub>2</sub>)AuCl). To this aim various bases and reaction conditions were tested (see Supporting Information).

Initially, LiHMDS, MeONa and *t*BuOK in combination with (NaphtDHD-Mes)HBF<sub>4</sub> (**2a**) afforded the desired (NaphtDHD-Mes)AuCl complex (**3a**) in poor to moderated yields (17–52%). K<sub>2</sub>CO<sub>3</sub> for instance, was not basic enough for the deprotonation according to <sup>1</sup>H NMR analysis of the crude mixture. By varying quantities of base and substrate, *t*BuOK was established as the optimal deprotonating base at -78°C (Scheme 1). Thus, the NHC precursors **2a–c** reacted with *t*BuOK in the presence of (SMe<sub>2</sub>)AuCl to afford the neutral complexes **3a–c** as colourless solids in 43–78% yield. Their structures were all confirmed by NMR, mass spectrometry and IR spectroscopy. These new gold complexes are readily soluble in CH<sub>2</sub>Cl<sub>2</sub>, CHCl<sub>3</sub>, acetone or THF but insoluble in diethyl ether, hexane and pentane.

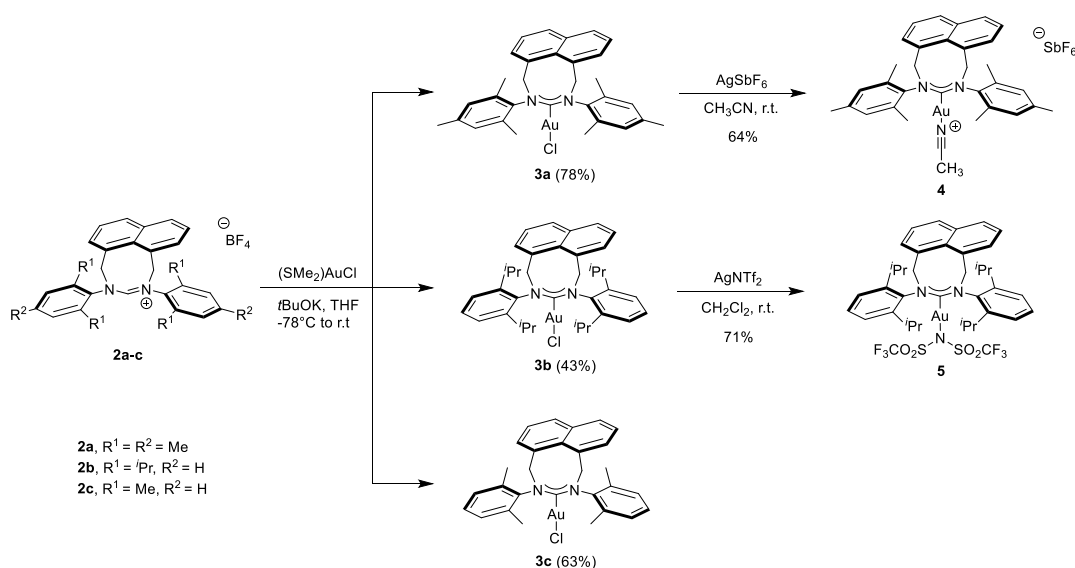
With the neutral NHC-Au(I) complexes in hand, we aimed on the synthesis of highly electron-deficient cationic complexes by anion metathesis using weakly coordinating counter anions. We envisaged

hexafluoroantimonate (SbF<sub>6</sub><sup>-</sup>) and triflimidate (NTf<sub>2</sub><sup>-</sup>), as suitable moieties for the synthesis of cationic NHC-Au(I) complexes.<sup>[15–17]</sup> To this end, the treatment of the gold(I) chloride complexes with 1 equivalent of either AgSbF<sub>6</sub> or AgNTf<sub>2</sub> was attempted (Scheme 1). The reaction of **3a** with AgSbF<sub>6</sub> in acetonitrile at room temperature afforded the cationic complex [(NaphtDHD-Mes)AuNCCH<sub>3</sub>]<sup>+</sup>SbF<sub>6</sub><sup>-</sup> (**4**) in 64% isolated yield as a colourless crystalline solid. By analogy, complex **5** was obtained by the reaction of **3b** with 1 equivalent AgNTf<sub>2</sub> in CH<sub>2</sub>Cl<sub>2</sub> at room temperature in 71% yield. Recrystallization of the crude products from CH<sub>2</sub>Cl<sub>2</sub>/pentane afforded pure, crystalline gold complexes.

### Spectroscopic analysis

The presence of NCCH<sub>3</sub> in the complex **4** was indicated by the infrared spectra and the complexation to gold was confirmed from the stretching frequency compared to non-coordinated acetonitrile. FTIR-ATR of neat **4** shows signals (ν<sub>C≡N</sub> 2332, 2306 cm<sup>-1</sup>) which are higher than those for NCCH<sub>3</sub> (ν<sub>C≡N</sub> 2254, 2293 cm<sup>-1</sup>) due to the change in the electronic configuration of the acetonitrile upon complexation.<sup>[18]</sup> This is expected since the electron donation from the lone pair of the NCCH<sub>3</sub> to the gold center removes weakly antibonding electrons from the σ orbital at the CN bond upon coordination, and therefore strengthening it and increasing its stretching frequency (ν<sub>C≡N</sub>).<sup>[17,19]</sup>

The presence of the triflimidate moiety (NTf<sub>2</sub><sup>-</sup>) in complex **5** was confirmed by the ν<sub>S=O</sub> (1398, 1195 cm<sup>-1</sup>) and ν<sub>C-F</sub> (1131 cm<sup>-1</sup>) bands.<sup>[20]</sup> The <sup>13</sup>C NMR chemical shifts are summarized in Table 1. The carbene carbon signal (C<sub>NHC</sub>) of the neutral complexes (**3a–c**) range between 195–197 ppm, about Δ7 ppm shifted downfield compared to their corresponding cationic congeners **4** and **5** (188–190 ppm).



**Scheme 1.** General formation of NHC-Au(I) species **3a–c** and **4–5**.

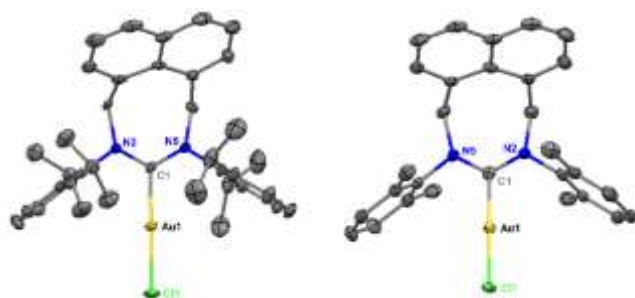
**Table 1.**  $^{13}\text{C}$  NMR shifts in neutral complexes (NHC)AuCl (**3**) and cationic species **4–5**.

Complex	$\text{C}_{\text{NHC}} \delta$ (ppm)	$\text{C}_Z \delta$ (ppm)
<b>3a</b> (NaphtDHD-Mes)AuCl	195.4	
<b>3b</b> (NaphtDHD-Dipp)AuCl	197.2	
<b>3c</b> (NaphtDHD-Xyl)AuCl	195.2	
<b>4</b> [(NaphtDHD-Mes)AuNCCH <sub>3</sub> ][SbF <sub>6</sub> ]	188.0	2.8 (C <sub>CH<sub>3</sub></sub> ), 119.6 (C <sub>CN</sub> )
<b>5</b> [(NaphtDHD-Dipp)AuNTf <sub>2</sub> ]	190.7	

In complex **4**, the carbon signals of acetonitrile are found at  $\delta(^{13}\text{C}) = 2.8$  ppm (C<sub>CH<sub>3</sub></sub>) and  $\delta(^{13}\text{C}) = 119.6$  ppm (C<sub>CN</sub>), which appeared slightly downfield shifted with respect to the non-coordinated acetonitrile [ $\delta(^{13}\text{C}) = 1.9$  ppm (C<sub>CH<sub>3</sub></sub>), 116.9 ppm (C<sub>CN</sub>)], indicating a net electron transfer from the coordinated NCCH<sub>3</sub> to the gold center.<sup>[19,21]</sup> The carbene carbon (C<sub>NHC</sub>) in **5** is apparent from the signal at  $\delta(^{13}\text{C}) = 190.7$  ppm, significantly highfield shifted with respect to that of the neutral species **3b** [ $\delta(^{13}\text{C}) = 197$  ppm] after halide abstraction. The  $^{19}\text{F}\{^1\text{H}\}$  NMR spectrum of complex **5** shows a singlet at  $\delta(^{19}\text{F}) = -74.5$  ppm corresponding to the CF<sub>3</sub> group (see Supporting Information).

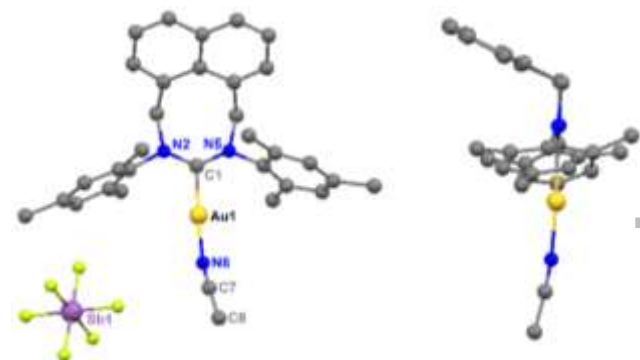
### Solid state structures and steric profiling

X-ray diffraction studies on single crystals of **3b** and **3c** confirmed the structures of the NHC gold(I) chloride complexes determined by NMR.<sup>[22]</sup> Suitable single crystals were obtained by slow evaporation of the solvent from a concentrated CH<sub>2</sub>Cl<sub>2</sub>/pentane solution of the complex at room temperature. The molecular structures are shown in Figure 1, and the selected crystallographic data are listed in Table 2.

**Figure 1.** Molecular structures of **3b** (left) and **3c** (right) in the solid state (ORTEP representations). Ellipsoids are drawn at 45% probability level and all hydrogen atoms are omitted for clarity.

Gratifyingly, slow evaporation of a solution of **4** in CH<sub>2</sub>Cl<sub>2</sub> led to the formation of a single crystal suitable for X-ray analysis (Figure 2). The presence of the counterion (SbF<sub>6</sub><sup>−</sup>) and the coordination of acetonitrile to the gold center were unequivocally established.<sup>[23]</sup> A colourless single crystal from **5** was grown by slow

diffusion of pentane into a concentrated solution of the complex in a CH<sub>2</sub>Cl<sub>2</sub>/CHCl<sub>3</sub> mixture followed by slow evaporation at room temperature overnight (Figure 3).<sup>[22]</sup> The N-C<sub>NHC</sub>-N angle in **5** (121.29(16)°) is marginally bigger than that in complex **3b** (121.2(4)°), revealing a negligible change in the molecular geometry of the NHC backbone after anion exchange from Cl<sup>−</sup> (**3b**) to NTf<sub>2</sub><sup>−</sup> (**5**). The C<sub>NHC</sub>-Au and Au-NTf<sub>2</sub> bond lengths in complex **5** are 2.004(18) Å and 2.1069(17) Å, respectively.

**Figure 2.** Ball-and-stick representation of cationic complex [(NaphtDHD-Mes)Au(NCMe)][SbF<sub>6</sub>] (**4**, left) and a side-view thought the N-C<sub>NHC</sub>-N plane (right). Hydrogen atoms are omitted for clarity.

The C<sub>NHC</sub>-Au-Cl bond angle found in **3b** (179.32(12)°) is almost linear, while the structure of **3c** showed a stronger deviation from linearity (173.88(13)°). Interestingly, both complexes exhibit broad N-C<sub>NHC</sub>-N angles (around 121°), which match those of other expanded-ring NHC-Au(I) complexes in the current literature.<sup>[13]</sup> The C<sub>NHC</sub>-Au (2.000(4)–2.002(5) Å) and Au-Cl (2.2955(1)–2.3158(12) Å) bond lengths lie in the range of other comparable expanded-ring NHC-Au(I) systems.<sup>[11,12,14]</sup>

**Table 2.** Selected structure and steric data of complexes **3b**, **3c** and **5**.

Complex	C <sub>NHC</sub> -Au (Å)	Au-X (Å)	C <sub>NHC</sub> -Au-X (°)	N-C <sub>NHC</sub> -N (°)	Torsion $\alpha$ (°) <sup>24</sup>	% V <sub>bur</sub> <sup>25</sup>
[(NaphtDHD-Dipp)AuCl] ( <b>3b</b> )	2.000(4)	2.2955(11)	179.32(12)	121.2(4)	30.9	54.0
[(NaphtDHD-Xyl)AuCl] ( <b>3c</b> )	2.002(5)	2.3158(12)	173.88(13)	121.3(5)	22.2	46.4
[(NaphtDHD-Dipp)AuNTf <sub>2</sub> ] ( <b>5</b> )	2.004(18)	2.1069(17)	177.90(7)	121.29(16)	49.4	51.6

The torsion angle  $\alpha$  (°) is a measurement of the spatial twisting of the *N*-aryl substituents around the C<sub>Ar</sub>---N<sub>2</sub>—N<sub>5</sub>---C<sub>Ar</sub>′ plane, with respect to the metal's coordination sphere.<sup>[24]</sup> The torsion angles found in **3b** ( $\alpha = 30.9^\circ$ ) and **3c** ( $\alpha = 22.2^\circ$ ) reveal the influence of the *ortho*-substituents in the *N*-aryls over the spatial arrangement of the complex. The bulky *ortho*-isopropyl substituents present in **3b** promote the twisting of the *N*-aryls resulting in an increased torsion angle while, comparatively, the *ortho*-methyl



substituents found in **3c** produce smaller impact on the twisting of the molecule. In addition, the naphthalene backbone exerts sharp influence on the *ortho*-substituents of the *N*-aryls by pushing them down towards the gold center. The solid state structure of **4** from a side-view (Figure 2, right) exhibits this effect. The twisting of both *N*-aryls is also visible from this privileged picture.

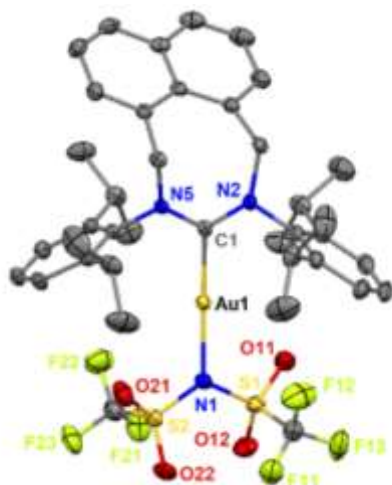


**Figure 3.** ORTEP representation of [(NaphtDHD-Dipp)AuNTf<sub>2</sub>] (**5**). Ellipsoids are drawn at 45% probability level. Hydrogen atoms and one CHCl<sub>3</sub> molecule were omitted for clarity.

The Topographic Steric Maps (TSM) and percent buried volume (% *V*<sub>bur</sub>) values were derived with help of the user-friendly interface (SambVca 2.0) developed by Cavallo *et al.* using the information from the CIF files of the X-ray diffraction analysis (Table 2).<sup>[25–27]</sup> Orange-to-red zones correspond to a more occupied (bulky) space while the green-to-blue areas represent the less bulky zones in the first coordination sphere of the gold center (Figure 4).

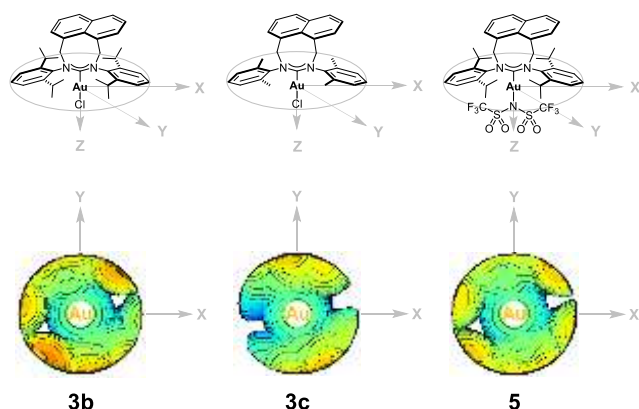


**Figure 4.** Steric maps of **3b**, **3c** and **5**.<sup>[28]</sup>

The TSM of **3b** confirms the above-mentioned twisting of the *N*-aryls with respect to the gold center;

while top-right and bottom-left corners are more occupied, a disproportionated steric distribution along the X axis can be noticed. This is associated to the molecular geometry of **3b**, in which two *ortho*-isopropyl substituents are relatively pointing down towards the gold center whereas the other two are pointing out of the sphere's first coordination of the complex. Analogously, the *ortho*-methyl substituents in complex **3c** leave some “free” or “uncovered” region (depicted along the X axis).

The counteranion (NTf<sub>2</sub><sup>-</sup>) in complex **5** exert high influence over two isopropyl groups of the *N*-aryls by pushing them out of the first coordination sphere of the gold center as evidenced by the increase in the torsion angle ( $\alpha = 49.4^\circ$ ) with respect to that of complex **3b** ( $\alpha = 30.9^\circ$ ). This steric re-distribution can easily be appreciated when comparing the steric maps of both **3b** and **5**, and particularly focusing on the top-right and bottom-left corners. While the steric map of **3b** reveals those bulky corners (orange), the analogous ones in **5** seem to be less occupied (yellow). The diminished % *V*<sub>bur</sub> value of **5** (51.6%) with respect to **3b** (% *V*<sub>bur</sub> = 54.0%) proves numerically the influence of the triflimidate moiety in the steric bulkiness of the gold complex after halide abstraction.

### Catalytic studies: Cycloisomerization of 1,6-Enynes

Gold complexes are excellent catalysts for the cyclization of a variety of enynes.<sup>[29]</sup> This divergent transformation has been examined in the presence of phosphine-, phosphite- and NHC-based catalysts due to the growing applicability in the synthesis of complex molecules.<sup>[30–33]</sup>

In the initial catalytic studies, we tested enyne **6a** as benchmark substrate under open-air conditions in non-anhydrous CH<sub>2</sub>Cl<sub>2</sub> by varying reaction times and temperature. The results using complexes **3a–c** as pre-catalysts and the cationic species **4** and **5** are summarized in Table 3. The cyclization of **6a** proceeded in >99% conversion within 15 minutes at room temperature in the presence of the complexes **3a–c** activated by AgSbF<sub>6</sub> to give a mixture of products **7–9** (Entries 1–3). Despite the unselective transformation under the given conditions, it is worth mentioning that a 1.0 mol% loading was able to promote the conversion almost completely in only a few minutes. Echavarren *et al.* reported that the phosphine donor gold complexes are efficient catalyst at the 2.0–5.0 mol% loading in comparative reaction times.<sup>[34]</sup>

**Table 3.** Exploration of cycloisomerization conditions<sup>a</sup>

Entry	[Au] cat	<i>T</i> [°C]	<i>t</i> [min]	Reaction	
				6a	7a, 8a, 9a
1	<b>3a</b> + AgSbF <sub>6</sub>	23	15	>99	1/0.6/1
2	<b>3b</b> + AgSbF <sub>6</sub>	23	15	>99	0.5/0.6/1
3	<b>3c</b> + AgSbF <sub>6</sub>	23	15	>99	0.3/0.6/1

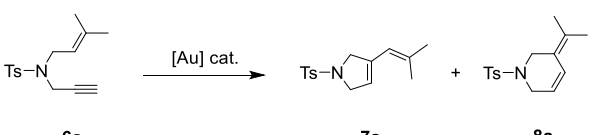
4	<b>3a</b> + AgSbF <sub>6</sub>	0	20	>99	1/0.5/0.9
5	<b>3b</b> + AgSbF <sub>6</sub>	0	20	>99	0.3/1/0.6
6 <sup>d</sup>	<b>4</b>	0	30	>99	1/0.1/0.1
7 <sup>d</sup>	<b>5</b>	0	15	>99	0.6/1/0.1

<sup>a)</sup> Reaction conditions: **6a** (0.2 mmol), [Au] cat. (2.0 mol%), CH<sub>2</sub>Cl<sub>2</sub> (2.0 mL), 23°C. <sup>b)</sup> Determined by <sup>1</sup>H NMR analysis.

<sup>c)</sup> Determined by GC-MS analysis. <sup>d)</sup> 0.5 mol% catalyst loading was used.

The formation of product **9a** can be explained by water addition to the intermediate cation/carbene.<sup>[33]</sup> When we settled the reaction at 0°C, by using complex **3a**, no significant variation of the result was observed (Entry 4). In addition, the transformation of **3b** at same temperature remained unselective (Entry 5). Importantly, the use of complexes **4** and **5**, considerably improved the selectivity, even under “wet” conditions, affording **7a** (Entry 6) and **8a** (Entry 7) as the main products, respectively. Moreover, a lower catalyst loading of the cationic species **4–5** (0.5 mol%) was enough to promote full conversion of the substrate after 15–30 minutes. By setting up the test reaction under anhydrous conditions (Table 4), only products **7a** and **8a** were formed. In all cases 99% conversion was achieved within 15 minutes. In the presence of **3b** a mixture of products was observed [**7a** (67) : **8a** (32), Entry 1]. The formation of the main product **7a** fits within the general *exo*-type mechanism followed by a single cleavage of the gold-carbene intermediate. No significant difference on the regioselectivity was observed by employing the cationic gold catalyst **4** [**7a** (64) : **8a** (35), Entry 3]. In contrast, the treatment of **6a** with a catalytic 1:1 mixture of **3b** and AgSbF<sub>6</sub> produced almost exclusively the *endo*-type single cleavage product **8a** (99%, Entry 2).

**Table 4.** Skeletal rearrangement of enyne **6a**<sup>a</sup>



Entry	Catalyst	Conversion (%) <sup>b</sup>	Products (Yield[%]) <sup>c</sup>
1	<b>3a</b> + AgSbF <sub>6</sub>	>99	<b>7a</b> (67) + <b>8a</b> (32)
2	<b>3b</b> + AgSbF <sub>6</sub>	>99	<b>8a</b> (99)
3	<b>4</b>	>99	<b>7a</b> (64) + <b>8a</b> (35)
4	<b>5</b>	>99	<b>7a</b> (28) + <b>8a</b> (71)

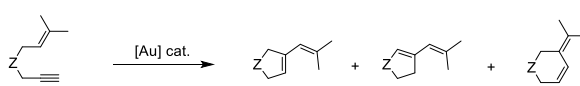
<sup>a)</sup> Reaction conditions: **6a** (0.1 mmol), [Au] catalyst (2 mol%), anhydrous CH<sub>2</sub>Cl<sub>2</sub>, 23°C, 15 min. <sup>b)</sup> Determined by <sup>1</sup>H NMR analysis. <sup>c)</sup> Determined by GC-MS analysis.

To our surprise, the employment of cationic complex **5** led to a decrease in the selectivity of the reaction, yielding a mixture of *endo* : *exo* products (71:28, Entry 4), despite a full conversion.

We then extended our study on other enyne systems. Therefore, substrates **6b** and **6c** were treated under the conditions mentioned below, using complexes **3a** or

**3b**, in the presence of AgSbF<sub>6</sub> as the activator (Table 5). Catalyst **3a** afforded a minor quantity of the *endo*-product **8** (3–10%, Entries 1 and 3) and predominantly the *exo*-product **7** (88–94%) for both substrates, accompanied by some traces of dienes **7b'** and **7c'** (2–3%) which could be detected by <sup>1</sup>H NMR analysis. The bulkier complex **3b** afforded no *endo*-product (**8**) and a mixture of isomers **7** appeared after 45 minutes (Entries 2 and 4). Interestingly, complex **3b** yielded a 1:1 mixture of only the isomers **7b** and **7b'** after 2 hours (see Supporting Information) with no traces of product **8b**. Similar product distribution was reported by Fensterbank *et al.* by using phosphine oxide-based gold(I) complexes which afforded a mixture of isomers [**7b** (88) : **7b'** (7)] upon 2 hours reaction, and by Echavarren *et al.* by using some phosphine-gold(I) complexes.<sup>[35,36]</sup>

**Table 5.** Skeletal rearrangement of enynes **6b** and **6c**<sup>a</sup>

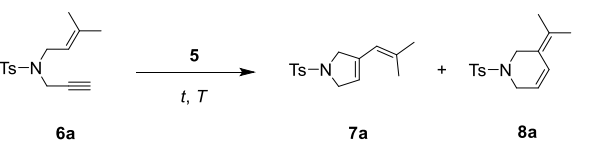


Entry	Enyne	Catalyst	Products (Yield[%]) <sup>b</sup>
1	<b>6b</b>	<b>3a</b> + AgSbF <sub>6</sub>	<b>7b</b> (94) + <b>7b'</b> (3) + <b>8b</b> (3)
2	<b>6b</b>	<b>3b</b> + AgSbF <sub>6</sub>	<b>7b</b> (66) + <b>7b'</b> (34)
3	<b>6c</b>	<b>3a</b> + AgSbF <sub>6</sub>	<b>7c</b> (88) + <b>7c'</b> (2) + <b>8c</b> (10)
4	<b>6c</b>	<b>3b</b> + AgSbF <sub>6</sub>	<b>7c</b> (90) + <b>7c'</b> (10)

<sup>a)</sup> Reaction conditions: **6** (0.1 mmol), [Au] catalyst (2 mol%), anhydrous CH<sub>2</sub>Cl<sub>2</sub>, 23°C, 45 min. <sup>b)</sup> Determined by <sup>1</sup>H NMR analysis.

Subsequently, the performance of complex **5** was investigated at lower catalyst loadings (Table 6). 0.25 mol% loading afforded a combined yield of 92% after 1 hour (Entry 1). When the loadings were diminished to 0.15–0.10 mol%, the yields proportionally decreased (65–41%, Entries 2 and 3, respectively). After 12 hours, 0.05 mol% of catalyst afforded 37% yield (Entry 5), slightly higher than that after 1 hour (29%, Entry 4). An 11% yield was observed after 12 hours using 0.01 mol% catalyst loading (TON = 1100, Entry 7) while a 0.005 mol% loading provided 7% yield after 24 hours (TON = 1400, Entry 9) which proves that the gold complex remained catalytically active in solution after several hours.

**Table 6.** Efficiency of cationic complex **5** on the cyclization of enyne **6a**<sup>a</sup>



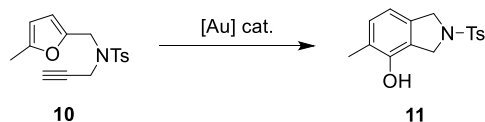
Entry	<b>5</b> (mol%)	t [h]	<b>7+8</b> (%) <sup>b</sup>	TON	TOF (h <sup>-1</sup> )
1	0.250	1	92	368	368

2	0.150	1	65	433	433
3	0.100	1	41	410	410
4	0.050	1	29	580	580
5	0.050	12	37	740	62
6	0.025	12	16	640	53
7	0.010	12	11	1100	92
8	0.005	12	4	800	67
9	0.005	24	7	1400	66

<sup>a</sup>) Reaction conditions: **6a** (50  $\mu$ mol), **5** (0.005–0.250 mol%), anhydrous  $\text{CH}_2\text{Cl}_2$  (0.05 M), 0°C. <sup>b</sup>) Determined by GC-MS analysis using dodecane as the internal standard.

Next the activity of the complexes was evaluated in the gold-catalyzed synthesis of phenols, by using substituted furane **10** as the substrate and 5 mol% catalyst at the 50  $\mu$ mol scale.<sup>[37]</sup> As indicated in Table 7, the pre-catalysts **3a**, **3b** and **3c** afforded moderated to good yields (55–89%, Entries 1–3) whereas the active gold catalysts **4** and **5** yielded 97% and 99% respectively, under the same reaction conditions (Entries 4 and 5).

**Table 7.** Gold-catalyzed phenol synthesis<sup>a</sup>



Entry	Catalyst	Yield (%) <sup>b</sup>
1	<b>3a</b> + AgNTf <sub>2</sub>	69
2	<b>3b</b> + AgNTf <sub>2</sub>	55
3	<b>3c</b> + AgNTf <sub>2</sub>	89
4	<b>4</b>	97
5	<b>5</b>	99

<sup>a</sup>) Reaction conditions: **10** (15.3 mg, 50  $\mu$ mol), [Au] cat (5.0 mol%), AgNTf<sub>2</sub> (5.0 mol%), Diphenylmethane (8.3 mg, 50  $\mu$ mol; internal standard),  $\text{CDCl}_3$  (0.5 mL), 23°C, 2 h. <sup>b</sup>) Determined by <sup>1</sup>H NMR analysis.

Interestingly, the sterically demanding complex **3b** (%  $V_{\text{bur}}$  = 54.0) resulted less active than **3c** (%  $V_{\text{bur}}$  = 46.4) on this transformation affording only 55% yield. Given that catalyst **5** afforded an excellent yield (99%), the results from the in situ activated pre-catalyst **3b** could be misleading, since the adventitious  $\text{Ag}^+$  (from the NHC-AuCl activation) might intercept key organogold intermediates and affect negatively the catalysis.<sup>[38,39]</sup>

Finally, we assessed the (NaphtDHD-Dipp)Au<sup>+</sup>NTf<sub>2</sub><sup>-</sup> species to ascertain the catalytic activity of either the pre-formed catalyst or the in situ-activated gold complex.<sup>[40]</sup> For direct comparison, **5** and the system **3b** + AgNTf<sub>2</sub> were employed in the cycloisomerization of *N*-propargyl carboxamide **12** as the case reaction (Figure 5). The conversion to form oxazoline **13** proceeded in 99% conversion after ca. 5 hours in the

presence of catalyst **5**, while pre-catalyst **3b** activated with 1 equivalent AgNTf<sub>2</sub> was found to be slightly slower, but active enough to reach a full conversion after 7.5 hours. For both catalytic systems, the reaction followed first-order kinetics until 99% conversion along 5 hours and 7.5 hours, respectively.

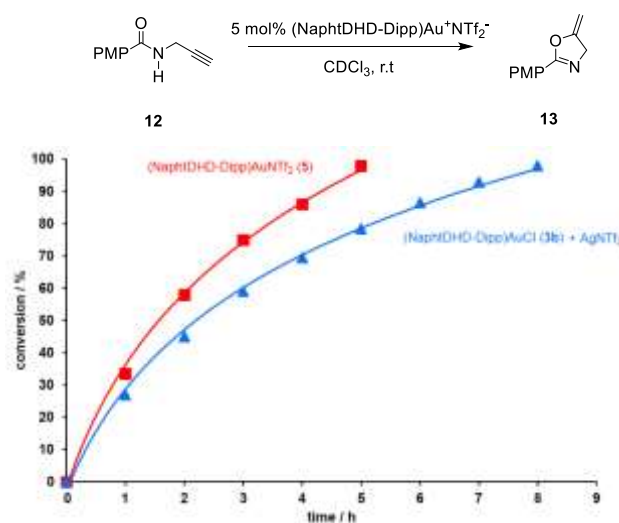


**Figure 5.** Cycloisomerization of *N*-propargyl carboxamide **12** to oxazoline **13** catalyzed by (NaphtDHD-Dipp)Au<sup>+</sup>NTf<sub>2</sub><sup>-</sup> species.

## Conclusion

Efficient, and in some cases highly selective, catalysts for the cycloisomerization of 1,6-enynes have been synthesized using sterically demanding eight-membered NHC ligands. This library of gold(I) complexes has been fully characterized and the solid-state structures have confirmed their structures as well as their steric properties.

The X-ray diffraction analysis revealed broad N-C<sub>NHC</sub>-N angles (around 121°) and torsion angles between 12° and 31° which are directly related to steric environment around the gold center (%  $V_{\text{bur}}$  = 46–54%). The catalytic performance of the complexes has been evaluated at the 2 mol% loadings in the cycloisomerization of 1,6-enynes obtaining full conversions in all cases. The activity of cationic complex **5** was tested down to 0.005 mol% loading yielding 7% combined product after 24 hours.

In the skeletal rearrangement of **6a** the pre-catalyst **3b** afforded 99% conversion and excellent selectivity (*endo* : *exo* = 99:1) after several minutes using 2 mol% catalyst loading. In the presence of this sterically demanding complex, the reaction proceeded via *endo*-type single cleavage to give almost exclusively the product **8a**. The selectivity of the reaction is considerably diminished using complex **3a** and cationic species **4** and **5** (*endo* = 32–71; *exo* = 28–67) despite full conversions were observed under the studied conditions.

In the latter, a comparative kinetic experiment on the cyclization of a *N*-propargyl carboxamide

demonstrated no significant difference between the performance of the active gold species (NaphtDHD-Dipp)Au<sup>+</sup>NTf<sub>2</sub><sup>-</sup> generated either by in situ activation (**3b** + AgNTf<sub>2</sub>) or from the preformed gold catalyst **5**. With the results discussed above, this library of neutral and cationic NHC-Au(I) complexes shows a tremendous potential to be employed as catalysts on several other gold(I)-catalyzed transformations.

## Experimental Section

Unless otherwise stated, the synthesis of gold complexes was carried out using standard Schlenk techniques using dry solvents dispensed from MB SPS 800 solvent system or inside an argon-filled glove box when needed. Organogold compounds were stored under an atmosphere of dry nitrogen at low temperature (*ca.* -35°C) after syntheses to avoid decomposition. THF was degassed by Freeze-Pump-Thaw prior to use. NMR characterization data was collected at 296 K at the department of chemistry of the University of Heidelberg in Bruker Avance DRX 300 (300 MHz), Bruker Avance III 400 (400 MHz), Bruker Avance III 500 (500 MHz) and Bruker Avance III 600 (600 MHz). <sup>1</sup>H and <sup>13</sup>C spectra are given relative to TMS (0.00 ppm) or to the residual protons in deuterated solvents (CD<sub>2</sub>Cl<sub>2</sub>: 5.32 ppm, 53.84 ppm; and CDCl<sub>3</sub>: 7.26 ppm, 77.16 ppm). Melting points were determined in a BÜCHI automated B-545 apparatus and are uncorrected. High resolution mass spectra (HRMS) were recorded on a Bruker Apex-Qe hybrid 9.4 FT- ICR spectrometer (ESI<sup>+</sup>, MALDI). IR spectra were recorded on a Bruker Vector 22 Lumos FT- IR. UV-Vis were accomplished in a V-670 UV-VIS-NIR Spectrophotometer. NHC-HBF<sub>4</sub> salts were prepared according to literature.<sup>[12c]</sup>

### General procedure for the synthesis of NHC-AuCl complexes 3a-c

A 4.5 mL screw-cap vial provided with stirring bar, was charged with NHC-HBF<sub>4</sub> salt (0.10 mmol), DMS-AuCl (0.05 mmol, 0.5 equiv.), *t*-BuOK (0.165 mmol, 1.65 equiv) and 4A MS (30 mg) under open-air conditions at room temperature. Vial was sealed with Teflon/silicone septa and purged-back filled with nitrogen three times. After cooling to -78°C in dry ice-acetone bath, dry degassed THF (3 mL) was introduced to vial with a syringe and suspension was stirred overnight, allowing to warm up slowly to room temperature. Dark suspension was directly passed through a pad of silica gel (1.5 x 3 cm), followed by washing the pad with anhydrous CH<sub>2</sub>Cl<sub>2</sub> (10 mL). The solvent was removed in vacuo till a minimal volume followed by addition of *n*-hexane (*ca.* 40 mL). The precipitated gold complex was allowed to settle for 1 hour and the supernatant liquid was decanted off, the solid residue was washed with *n*-hexane and dried. Pure gold complexes are obtained as colorless solids after recrystallization from CH<sub>2</sub>Cl<sub>2</sub>:pentane mixture or by flash chromatography (ALOX, CH<sub>2</sub>Cl<sub>2</sub>/P.E, 4:1).

**(NaptDHD-Mes)AuCl (3a).** Yield: 52 mg (78%); m.p: 266–268 °C; <sup>1</sup>H NMR (500 MHz, CDCl<sub>3</sub>) δ 7.88 (d, *J* = 8.1 Hz, 2H), 7.46 – 7.27 (m, 2H), 7.14 (d, *J* = 6.9 Hz, 2H), 6.90 (s, 2H), 6.71 (s, 2H), 6.37 (d, *J* = 16.0 Hz, 2H), 4.42 (d, *J* = 16.0 Hz, 2H), 2.37 (s, 6H), 2.19 (s, 6H), 1.40 (s, 6H); <sup>13</sup>C NMR (126 MHz, CDCl<sub>3</sub>) δ 195.35, 145.37, 137.84, 135.19,

134.43, 133.78, 132.42, 131.53, 131.48, 130.75, 130.00, 129.88, 125.94, 58.03, 21.10, 18.52, 18.30; IR (ATR, cm<sup>-1</sup>):  $\nu_{\max}$  = 2978, 2856, 1476, 1440, 1308, 1037, 877, 824, 686; UV-vis (CH<sub>2</sub>Cl<sub>2</sub>) λ (log ε): 279 (3.82), 289 (3.84), 299 (3.68), 316 (2.79) nm; HR-MS (ESI): calc. C<sub>31</sub>H<sub>32</sub>AuClN<sub>2</sub>Na [M+Na]<sup>+</sup> = 687.1812, found: 687.1829.

**(NaphtDHD-Dipp)AuCl (3b).** Yield: 32 mg (43%); m.p: >300 °C; <sup>1</sup>H NMR (500 MHz, CDCl<sub>3</sub>) δ 7.89 (d, *J* = 8.2 Hz, 2H), 7.39 (t, *J* = 7.6 Hz, 2H), 7.28 (t, *J* = 7.8 Hz, 2H), 7.25 (d, *J* = 7.1 Hz, 2H), 7.17 (dd, *J* = 7.7, 1.2 Hz, 2H), 7.05 – 6.95 (m, 2H), 6.28 (d, *J* = 16.0 Hz, 2H), 4.56 (d, *J* = 16.0 Hz, 2H), 3.16 (dt, *J* = 13.6, 6.8 Hz, 2H), 2.24 (dt, *J* = 13.5, 6.7 Hz, 2H), 1.41 (d, *J* = 6.7 Hz, 6H), 1.40 (d, *J* = 6.8 Hz, 6H), 1.07 (d, *J* = 6.8 Hz, 6H), 0.56 (d, *J* = 6.7 Hz, 6H); <sup>13</sup>C NMR (126 MHz, CDCl<sub>3</sub>) δ 197.17, 145.50, 144.99, 143.86, 135.12, 131.73, 131.68, 131.19, 130.95, 129.27, 125.88, 124.93, 124.87, 59.62, 29.30, 28.16, 25.37, 24.91, 24.80, 23.86. IR (ATR, cm<sup>-1</sup>):  $\nu_{\max}$  = 2964, 2866, 1505, 1447, 1324, 1055, 823, 793; UV-vis (CH<sub>2</sub>Cl<sub>2</sub>) λ (log ε): 278 (3.90), 289 (3.92), 299 (3.94), 315 (2.91) nm; HR-MS (ESI): calc. C<sub>37</sub>H<sub>44</sub>AuClN<sub>2</sub>Na [M+Na]<sup>+</sup> = 771.2751, found: 771.2762.

**(NaphtDHD-Xyl)AuCl (3c).** Yield: 37 mg (63%); m.p: 231 °C; <sup>1</sup>H NMR (500 MHz, CDCl<sub>3</sub>) δ 7.90 (d, *J* = 8.2 Hz, 1H), 7.38 (t, *J* = 7.6 Hz, 1H), 7.14 (d, *J* = 7.0 Hz, 1H), 7.11 (d, *J* = 4.9 Hz, 2H), 6.92 (t, *J* = 4.5 Hz, 1H), 6.41 (d, *J* = 16.0 Hz, 1H), 2.42 (s, 3H), 1.46 (s, 3H); <sup>13</sup>C NMR (126 MHz, CDCl<sub>3</sub>) δ 195.23, 147.66, 135.25, 134.85, 134.21, 132.32, 131.60, 131.40, 130.88, 129.31, 128.41, 125.99, 57.90, 18.62, 18.41; IR (ATR, cm<sup>-1</sup>):  $\nu_{\max}$  = 3043, 2953, 2852, 1509, 1470, 1305, 1170, 823, 771, 684. UV-vis (CH<sub>2</sub>Cl<sub>2</sub>) λ (log ε): 269 (4.98), 279 (4.90), 289 (4.90), 299 (4.77), 316 (3.72) nm; HR-MS (ESI): calc. C<sub>31</sub>H<sub>32</sub>AuClN<sub>2</sub>Na [M+Na]<sup>+</sup> = 659.1499, found: 659.1513.

**[(NaptDHD-Mes)AuNCCH<sub>3</sub>]SbF<sub>6</sub> (4).** Inside the glove box, a 4.5 mL amber screw-cap Teflon coated vial provided with stirring bar, was charged with gold(I)-chloride complex **3a** (50 mg, 0.075 mmol) and AgSbF<sub>6</sub> (26 mg, 0.075 mmol, 1.0 equiv). The vial was taken out of the glove box and anhydrous MeCN (1.0 mL) was added to the mixture via syringe. The suspension was stirred at room temperature for 4.5 hours and filtered through a short plug of Celite to remove solid impurities and the solvent was removed *in vacuo*. The oily residue was taken up in anhydrous CH<sub>2</sub>Cl<sub>2</sub> (1 mL) and diethyl ether was added dropwise to solution until a colorless precipitate appeared. The suspension kept on the bench for 15 minutes in dark and solvent was removed via syringe. The crude product was recrystallized with CH<sub>2</sub>Cl<sub>2</sub>/pentane mixture and dried in vacuum to afford 44 mg (64%) of **4** as a colorless solid. m.p: 176 °C; <sup>1</sup>H NMR (600 MHz, CD<sub>2</sub>Cl<sub>2</sub>) δ 7.92 (d, *J* = 8.3 Hz, 2H), 7.38 (t, *J* = 7.6 Hz, 2H), 7.14 (d, *J* = 7.0 Hz, 2H), 6.98 (s, 2H), 6.76 (s, 2H), 6.43 (d, *J* = 16.1 Hz, 2H), 4.46 (d, *J* = 16.1 Hz, 2H), 2.35 (s, 6H), 2.22 (s, 6H), 2.03 (s, 3H), 1.35 (s, 6H); <sup>13</sup>C NMR (151 MHz, CD<sub>2</sub>Cl<sub>2</sub>) δ 188.06, 144.71, 138.91, 134.45, 134.37, 131.88, 131.85, 131.13, 130.12, 129.83, 126.11, 119.57, 58.20, 20.80, 18.20, 18.06, 2.84; IR (ATR, cm<sup>-1</sup>):  $\nu_{\max}$  = 2920, 2856, 2332, 2306, 1609, 1523, 1475, 1379, 1358, 1335, 1312, 1188, 1144, 1039, 1005, 947, 854, 825, 791, 766, 654; HR-MS (ESI): calc. C<sub>33</sub>H<sub>35</sub>AuN<sub>3</sub> [M-SbF<sub>6</sub>]<sup>+</sup> = 670.2497, found: 670.2505.

**[(NaptDHD-Dipp)Au]NTf<sub>2</sub> (5).** To a stirred solution of AgNTf<sub>2</sub> (39 mg, 0.10 mmol) in CH<sub>2</sub>Cl<sub>2</sub> (2 mL) was added



gold(I)-chloride complex **3b** (78 mg, 0.10 mmol) and immediately a suspension was formed. The reaction mixture was stirred in dark at room temperature for 8 hours and filtered through a short plug of Celite. The solvent was removed under a steam vent of nitrogen until an oily residue was obtained. Precipitation of the product was effected by crashing out the residue with the spatula over cold pentane. The crude product was recrystallized with CH<sub>2</sub>Cl<sub>2</sub>/pentane mixture and dried in vacuum to afford 70 mg (71%) of **5** as a colorless solid. m.p: 192°C; <sup>1</sup>H NMR (500 MHz, CDCl<sub>3</sub>) δ 7.97 (d, *J* = 7.8 Hz, 2H), 7.49 – 7.45 (m, 2H), 7.37 – 7.31 (m, 4H), 7.26 (dd, *J* = 7.1, 1.9 Hz, 2H), 7.08 (dd, *J* = 7.7, 1.3 Hz, 2H), 6.37 (d, *J* = 16.0 Hz, 2H), 4.68 (d, *J* = 16.0 Hz, 2H), 3.24 – 3.14 (m, 1H), 2.33 – 2.23 (m, 2H), 1.47 (d, *J* = 6.8 Hz, 6H), 1.46 (d, *J* = 6.8 Hz, 6H), 1.09 (d, *J* = 6.8 Hz, 6H), 0.62 (d, *J* = 6.7 Hz, 6H). <sup>13</sup>C NMR (126 MHz, CDCl<sub>3</sub>) δ 190.86, 145.34, 144.96, 143.54, 135.19, 132.01, 131.77, 131.27, 130.85, 129.57, 126.09, 125.27, 125.23, 60.04, 29.45, 28.33, 25.39, 25.12, 24.37, 24.08. IR (ATR, cm<sup>-1</sup>): ν<sub>max</sub> = 2965, 2929, 2870, 1674, 1510, 1463, 1398, 1363, 1324, 1195, 1131, 1055, 951, 823, 803, 773, 653, 610. HR-MS (ESI): calc. C<sub>39</sub>H<sub>44</sub>AuF<sub>6</sub>N<sub>3</sub>O<sub>4</sub>S<sub>2</sub>Na [M-Na]<sup>+</sup> = 745.3438, found: 745.3428.

#### General procedure for the catalyzed cycloisomerization of 1,6-enynes

A screw-cap vial was charged with enyne (0.5 mmol), NHC-Au(I) complex and corresponding silver halide. The vial was sealed with a Teflon-coated septum and purged with nitrogen once. Anhydrous CH<sub>2</sub>Cl<sub>2</sub> (2 mL) was introduced to mixture and reaction was stirred for the given time and temperature (*vide supra*). Crude products were purified by column chromatography (SiO<sub>2</sub>, P.E 100%).

## Acknowledgements

A.C.R. is grateful for a Ph.D. fellowship from Consejo Nacional de Ciencia y Tecnología (México).

## References

- [1] A. J. Arduengo, R. L. Harlow, M. Kline, *J. Am. Chem. Soc.* **1991**, *113*, 361–363
- [2] a) R. Jazzar, H. Liang, B. Donnadieu, G. Bertrand, *J. Organometallic Chem.* **2006**, *691*, 3201–3205; b) A. Gómez-Suárez, D. J. Nelson, S. P. Nolan, *Chem. Commun.* **2017**, *53*, 2650–2660.
- [3] a) N. Phillips, R. Trifoin, S. Aldridge, *Chem. Eur. J.* **2014**, *20*, 3825; (b) H. V. Huynh, *Chem. Rev.* **2018**, *118*, 9457–9492.
- [4] a) E. L. Kolychev, I. A. Portnyagin, V. V. Shuntikov, V. N. Khrustalev, M. S. Nechaev, *J. Organomet. Chem.* **2009**, *694*, 2454–2462; b) A. Cervantes-Reyes, F. Rominger, A. S. K. Hashmi, *Chem. Eur. J.* **2010**, *16*, 14348–14353; c) J. J. Dunsford, B. M. Kariuki, *Organometallics* **2011**, *30*, 5649–5655; d) A. Kumar, D. Yuan, H. V. Huynh, *Inorg. Chem.* **2019**, *58*, 7545–7553.
- [5] a) M. Iglesias, D. J. Beetstra, J. C. Knight, L. L. Ooi, A. Stasch, S. Coles, L. Male, M. B. Hursthouse, K. J. Cavell, A. Dervisi, I. A. Fallis, *Organometallics* **2008**, *27*, 3279–3289.
- [6] a) N. Marion, S. P. Nolan, *Chem. Soc. Rev.* **2008**, *37*, 1776–1782; b) J. J. Dunsford, B. M. Kariuki, K. J. Cavell, *Organometallics* **2012**, *31*, 4118–4121.
- [7] a) G. Dyker, *Angew. Chem.* **2000**, *112*, 4407–4409; *Angew. Chem. Int. Ed.* **2000**, *39*, 4237–4239; b) A. S. K. Hashmi, *Gold. Bull.*, **2003**, *36*, 3–9; c) A. S. K. Hashmi, *Gold Bull.* **2004**, *37*, 51–65; d) N. Krause, A. Hoffmann-Röder, *Org. Biomol. Chem.* **2005**, *3*, 387–391; e) A. S. K. Hashmi, G. Hutchings, *Angew. Chem.* **2006**, *118*, 8064–8105; *Angew. Chem. Int. Ed.* **2006**, *45*, 7896–7936; f) D. J. Gorin, F. D. Toste, *Nature*, **2007**, *446*, 395–403; g) A. Fürstner, P. W. Davies, *Angew. Chem.* **2007**, *119*, 3478–3519; *Angew. Chem. Int. Ed.* **2007**, *46*, 3410–3449; h) E. Jimenez-Nunez, A. M. Echavarren, *Chem. Commun.* **2007**, 333–346; i) A. S. K. Hashmi, *Chem. Rev.* **2007**, *107*, 3180–3211; j) Z. Li, C. Brouwer, C. He, *Chem. Rev.* **2008**, *108*, 3239–3265; k) A. Arcadi, *Chem. Rev.* **2008**, *108*, 3266–3325; l) R. Skouta, C.-J. Li, *Tetrahedron* **2008**, *64*, 4917–4938; m) H. C. Shen, *Tetrahedron* **2008**, *64*, 3885–3903; n) H. C. Shen, *Tetrahedron* **2008**, *64*, 7847–7870; o) S. Sengupta, X. Shi, *ChemCatChem* **2010**, *2*, 609–619; p) A. Corma, A. Leyva-Pérez, M. J. Sabater, *Chem. Rev.* **2011**, *111*, 1657–1712; q) J. Xiao, X. Li, *Angew. Chem.* **2011**, *123*, 7364–7375; *Angew. Chem. Int. Ed.* **2011**, *50*, 7226–7236; r) C. Obradors, A. M. Echavarren, *Chem. Commun.* **2014**, *50*, 16; s) D. Pflästerer, A. S. K. Hashmi, *Chem. Soc. Rev.* **2016**, *45*, 1331–1367.
- [8] a) S. Flügge, A. Anoop, R. Goddard, W. Thiel, A. Fürstner, *Chem. Eur. J.* **2009**, *15*, 8558–8565; b) O. S. Morozov, A. V. Lunchev, A. A. Bush, A. A. Tukov, A. F. Asachenko, V. N. Khrustalev, S. S. Zaleskiy, V. P. Ananikov, M. S. Nechaev, *Chem. Eur. J.* **2014**, *20*, 6162–6170; c) N. Phillips, T. Dodson, R. Tirfoin, J. I. Bates, S. Aldridge, *Chem. Eur. J.* **2014**, *20*, 16721–16731.
- [9] a) Y.-C. Lee, S. Patil, C. Golz, C. Strohmann, S. Ziegler, K. Kumar, H. Waldmann, *Nat. Commun.* **2017**, *8*, 14043; b) Y.-C. Lee, K. Kumar, H. Waldmann, *Angew. Chem. Int. Ed.* **2018**, *57*, 5212–5226.
- [10] a) T. Wurm, F. Mulks, C. R. N. Böhlting, D. Riedel, P. Zargaran, M. Rudolph, F. Rominger, A. S. K. Hashmi, *Organometallics* **2016**, *35*, 1070–1078; b) K. R. Sampford, J. L. Carden, E. B. Kidner, A. Berry, K. J.

- Cavell, D. M. Murphy, B. M. Kariuki, P. D. Newman, *Dalton Trans.* **2019**, 48, 1850–1858.
- [12] For eight-membered NHC complexes of transition metals see: a) W. Y. Lu, K. J. Cavell, J. S. Wixey, B. Kariuki, *Organometallics* **2011**, 30, 5649–5655; b) M. J. Page, W. Y. Lu, R. C. Poulten, E. Carter, A. G. Algarra, B. M. Kariuki, S. A. Macgregor, M. F. Mahon, K. J. Cavell, D. M. Murphy, M. K. Whittlesey, *Chem. Eur. J.*, **2013**, 19, 2158–2167; c) G. A. Chesnokov, M. A. Topchiy, P. B. Dzhevakov, P. S. Gribanov, A. A. Tukov, V. N. Khrustalev, A. F. Asachenkob, N. S. Nechaev, *Dalton Trans.* **2017**, 46, 4331–4345; d) Q. Teng, W. Wu, H. A. Duong, H. V. Huynh, *Chem. Commun.* **2018**, 54, 6044–6047.
- [13] A. Kumar, C. Singh, H. Tinnermann, H. V. Huynh, *Organometallics* **2020**, 39, 172–181.
- [14] A. Cervantes-Reyes, F. Rominger, M. Rudolph, A. S. K. Hashmi, *Chem. Eur. J.* **2019**, 25, 11745–11757.
- [15] C. Bartolome, Z. Ramiro, M. N. Peñas-Defrutos, P. Espinet, *ACS Catal.* **2016**, 6, 6537–6545.
- [16]  $\text{NTf}_2^-$  has a weaker coordination ability than  $\text{TfO}^-$  or  $\text{ClO}_4^-$  see Ref. [2a].  $\text{SbF}_6^-$  can form dicoordinated mononuclear gold(I) species in presence of coordinating molecules (e.g.  $\text{NCCH}_3$ , THF, py) upon halide abstraction, see Ref. [15].
- [17] R. M. P. Veenboer, D. Gasperini, F. Nahra, D. B. Cordes, A. M. Slawin, C. S. J. Cazin, S. P. Nolan, *Organometallics* **2017**, 36, 3645–3653.
- [18] C. L. Angell, M. V. Howell, *J. Phys. Chem.* **1969**, 73, 2551–2554.
- [19] J. Yau, D. M. P. Mingos, *J. Chem. Soc., Dalton Trans.*, **1997**, 1103–1111.
- [20] N. Mézailles, L. Ricard, F. Gagosz, *Org. Lett.* **2005**, 7, 4133–4136.
- [21] G. R. Fulmer, A. J. M. Miller, N. H. Sherden, H. E. Gottlieb, A. Nudelman, B. M. Stoltz, J. E. Bercaw, K. I. Goldberg, *Organometallics* **2010**, 29, 2176–2179.
- [22] CCDC 1980438 (**3b**), 1980439 (**3c**) and 1980441 (**5**) contain the supplementary crystallographic data for this paper. These data can be obtained free of charge from The Cambridge Crystallographic Data Centre via [www.ccdc.cam.ac.uk/data\\_request/cif](http://www.ccdc.cam.ac.uk/data_request/cif).
- [23] Crystal data are not given for **4** in the main article, due to the poor structure model ( $R = 0.1303$ ). The structure obtained defines the connectivity and confirms the overall composition of **4**, but bond lengths and angles of the NHC complex are not reliably obtained from this crystal structure and are therefore not included in Table 2. The CIF file has been included in the Supporting Information.
- [24] For the torsion angle  $\alpha$  ( $^\circ$ ) in expanded-ring NHC systems: See Refs. [4b], [6], [14].
- [25] a) A. Poater, F. Ragone, S. Giudice, C. Costabile, R. Dorta, S. P. Nolan, L. Cavallo, *Organometallics* **2008**, 27, 2679–2681; b) H. Clavier, S. P. Nolan, *Chem. Commun.* **2010**, 46, 841–861.
- [26] a) P. De Frémont, N. M. Scott, E. D. Stevens, S. P. Nolan, *Organometallics* **2005**, 24, 2411–2418; b) A. Poater, L. Falivene, C. A. Urbina-Blanco, S. Manzini, S. P. Nolan, L. Cavallo, *Dalton Trans.* **2013**, 42, 7433–7439.
- [27] A. Poater, B. Cosenza, A. Correa, S. Giudice, F. Ragone, V. Scarano, L. Cavallo, *Eur. J. Inorg. Chem.* **2009**, 1759.
- [28] Settings for the calculation:  $r = 3.5 \text{ \AA}$  (radius of the sphere around the metal center),  $d = 2.0 \text{ \AA}$  (bond length  $\text{C}_{\text{NHC}}\text{--metal}$ ), Bondi radii scaled by 1.17 and a mesh spacing of  $0.10 \text{ \AA}$  was used to scan the sphere of the buried voxels. All hydrogens were omitted for the calculations.
- [29] a) C. Nieto-Oberhuber, M. P. Munoz, S. Lopez, E. Jimenez-Nunez, C. Nevado, E. Herrero-Gomez, M. Raducan, A. M. Echavarren, *Chem. Eur. J.* **2006**, 12, 1677–1693; b) B. D. Robertson, R. E. M. Brooner, R. A. Widenhoefer, *Chem. Eur. J.* **2015**, 21, 5714–5717.
- [30] a) Mézailles, N., Ricard, L.; Gagosz, F. *Org. Lett.* **2005**, 7, 19, 4133–4136; b) J. Dubarle-Offner, M. Barbazanges, M. Augé, C. Desmarests, J. Moussa, M. R. Axet, C. Ollivier, C. Aubert, L. Fensterbank, V. Gandon, M. Malacria, G. Gontard, H. Amouri, *Organometallics* **2013**, 32, 1665–1673; c) C. Vriamont, M. Devillers, O. Riant, S. Hermans, *Chem. Eur. J.* **2013**, 19, 12009–12017; d) M. Rigo, E. R. M. Habraken, K. Bhattacharyya, A. W. Ehlers, N. Mozailles, J. C. Slootweg, C. Müller, *Chem. Eur. J.* **2019**, 25, 1–12.
- [31] M. C. Blanco-Jaimes, F. Rominger, M. M. Pereira, R. M. B. Carrilho, S. A. C. Carabineiro, A. S. K. Hashmi, *Chem. Commun.* **2014**, 50, 4937–4940.
- [32] Y. Tang, I. Benaissa, M. Huynh, L. Vendier, N. Lugan, S. Bastin, P. Belmont, V. César, V. Michelet, *Angew. Chem. Int. Ed.* **2019**, 58, 7977–7981.
- [33] a) E. Jiménez-Núñez A. M. Echavarren. *Chem. Rev.* **2008**, 108, 3326–3350; b) R. Dorel, A. M. Echavarren, *Chem. Rev.* **2015**, 115, 9028–9072.
- [34] C. Nieto-Oberhuber, M. P. Muñoz, E. Buñuel, C. Nevado, D. J. Cárdenas, A. M. Echavarren, *Angew. Chem. Int. Ed.* **2004**, 43, 2402–2406.
- [35] F. Schröder, C. Tugny, E. Salanouve, H. Clavier, L. Giordano, D. Moraleda, Y. Gimbert, V. Mouriès-Mansuy, J.-P. Goddard, L. Fensterbank, *Organometallics* **2014**, 33, 4051–4056.
- [36] S. Ferrer, A. M. Echavarren, *Organometallics* **2018**, 37, 781–786.
- [37] a) A. S. K. Hashmi, T. M. Frost, J. W. Bats, *J. Am. Chem. Soc.* **2000**, 122, 11553–11554; b) T. M. Frost, J. W. Bats, A. S. K. Hashmi, *Org. Lett.* **2001**, 3, 3769–3771.

- [38] Weber, M. R. Gagné, *Org. Lett.* **2009**, *11*, 4962–4965.
- [39] Wang, R. Cai, S. Sharma, J. Jirak, S. K. Thummanapelli, N. G. Akhmedov, H. Zhang, X. Liu, J. L. Petersen, X. Shi, *J. Am. Chem. Soc.* **2012**, *134*, 9012–9019.
- [40] Lu, J. Han, G. B. Hammond, B. Xu, *Org. Lett.* **2015**, *17*, 4534–4537.

## UPDATE

**Gold(I) Complexes with Eight-Membered NHC Ligands: Synthesis, Structures and Catalytic Activity***Adv. Synth. Catal.* **Year**, *Volume*, Page – PageA. Cervantes-Reyes, F. Rominger, M. Rudolph,  
A. Stephen K. Hashmi\*